Am J Transl Res 2025;17(2):1178-1199
www.ajtr.org /ISSN:1943-8141/AJTR0161613

Original Article

Magnesium cantharidate inhibits hepatocellular cancer by targeting RACK1

Da Sun[1], Xiaofei Li[1,2], Meichen Liu[1], Zhenfu Chen[1], Lingjun Wang[1], Rong Yan[1,2]

[1]College of Basic Medicine, Zunyi Medical University, Zunyi 563000, Guizhou, China; [2]Guizhou Provincial College-Based Key Lab for Tumor Prevention and Treatment with Distinctive Medicines, Zunyi Medical University, Zunyi 563000, Guizhou, China

Received October 31, 2024; Accepted January 22, 2025; Epub February 15, 2025; Published February 28, 2025

Abstract: Objective: The aim of this study was to investigate whether magnesium cantharidate (MC) exerts anti-hepatocellular carcinoma (anti-HCC) effects by targeting receptor for activated C kinase 1 (RACK1). Methods: The Cancer Genome Atlas (TCGA) database was used to analyze the expression of RACK1 in liver tissues. Molecular docking was used to examine the binding interactions between MC and RACK1. Huh-7 and SK-Hep-1 liver cancer cells' viability, proliferation, and apoptosis were assessed by using the Cell Counting Kit-8 (CCK-8) assay, 5-ethynyl-2'-deoxyuridine (EdU), and flow cytometry, respectively. RNA sequencing was used to explore the underlying mechanisms. Quantitative real-time PCR, immunohistochemistry, and western blotting were performed to explore the expression of key genes and proteins. Results: TCGA analysis revealed significant upregulation of RACK1 in liver cancer tissues that was correlated with tissue type, grade, TP53 mutation, and overall survival. Molecular docking results revealed that the minimum binding energy between MC and RACK1 was -5.8 kcal/mol. Moreover, RACK1 overexpression significantly promoted cell viability and proliferation, and inhibited apoptosis in liver cancer cells. However, MC significantly reversed the viability, proliferation, and apoptosis effects induced by RACK1 overexpression in liver cancer cells. MC significantly inhibited the growth of subcutaneously transplanted tumors *in vivo*. RNA sequencing revealed that MC inhibited proliferation and apoptosis by targeting RACK1 to regulate calcium ion transport, ion channels, and cell adhesion in liver cancer cells. Conclusion: MC exerts anti-HCC effects by targeting RACK1.

Keywords: Magnesium cantharidate, receptor for activated c kinase 1, hepatocellular carcinoma, proliferation, apoptosis

Introduction

Liver cancer is a highly aggressive malignant tumor characterized by rapid progression, shorter patient survival, higher lethality, challenging treatment choices, and pronounced tendency to recur and metastasize postoperatively. According to 2022 global cancer statistics, liver cancer accounts for 4.7% of the global incidence of all cancers and contributes to 8.2% of the global mortality rate [1]. Hepatocellular carcinoma (HCC) accounts for 75%-85% of all liver cancer cases [2]. The current clinical treatments for liver cancer primarily involve surgery, radiotherapy, and chemotherapy. However, elusive early stage symptoms make an early diagnosis challenging, thereby leading to diagnoses that often occur in advanced stages of metastasis [3]. Additionally, the lack of effective therapeutic drugs and methods results in a high recurrence rate, even after surgical resection. Clinical treatment outcomes for liver cancer consequently remain unsatisfactory.

Receptor for activated C kinase 1 (RACK1), also called guanine nucleotide-binding protein β-2-like 1 (GNB2L1), is a highly conserved DW40 repeat protein that facilitates the accumulation of different factors in ribosomes and directs them to diverse subcellular locations [4]. Extensive studies have demonstrated that RACK1 is involved in several cellular functions such as transmembrane transporter protein activity, ribosome activity, autophagy, proliferation, and apoptosis [5]. RACK1 promotes tumor progression by modulating certain signaling pathways such as Src/FAK [6], Iκκ/NFκB [7], and Wnt/β-catenin

https://doi.org/10.62347/PGAK3727

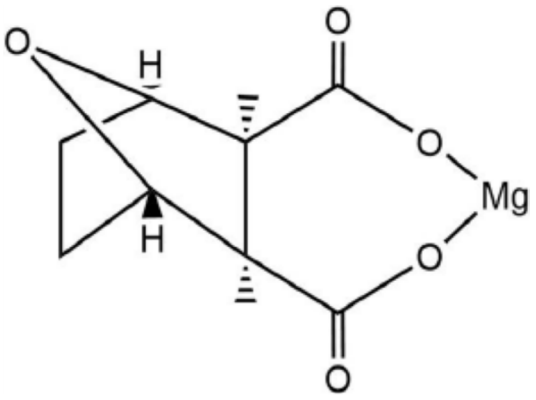

Figure 1. Chemical structures of magnesium cantharidate (MC).

pathways [8]. Aberrant RACK1 expression is associated with various cancers, including breast [9], pancreatic [10], gastric [11], and liver cancers [12], thereby making RACK1 a possible target for cancer therapies. A previous study reports that RACK1 expression is significantly upregulated in clinical HCC tissues [13]. Moreover, RACK1 enhances the proliferation, migration, and invasion capabilities of mouse HCC cell lines Hca-P and Hca-F [14]. Silencing RACK1, conversely, induces apoptosis and inhibits cell proliferation in hepatocellular carcinoma MHCC97-H cells [15]. These findings highlight the close association between RACK1 expression and HCC progression.

Active ingredients in traditional herbs exhibit diverse biologic effects such as immunological competence and anticancer properties. Cantharidin, derived from the medicinal insect *Cantharis*, has shown excellent effects in suppressing proliferation and inducing apoptosis in liver cancer cells [16, 17]. An Aidi injection derived from Cantharis also exhibits commendable anti-HCC effects [18, 19]. Magnesium cantharidate (MC) is a cantharidate compound found in *Cantharis*. The molecular formula of MC is $C_{10}H_{12}O_5Mg$ (**Figure 1**). Compared to cantharidin, MC has lower toxicity and better developmental potential. Of note, our previous study demonstrated that MC inhibits the proliferation of human hepatoma SMMC-7721 cells by inhibiting the mitogen-activated protein kinase (MAPK) signaling pathway [20]. Studies investigating the mechanisms underlying the anti-HCC effects of MC are regrettably limited, compared to the anti-HCC effects of other anti-HCC drugs, which restricts the clinical application of MC. Our previous RNA sequencing results revealed that MC treatment significantly downregulated the expression of RACK1 in the human hepatoma cell line SMMC-7721 [21]. However, no studies have reported whether MC inhibits HCC by inhibiting the expression of RACK1. Exploring whether MC exerts its anti-HCC effects through RACK1 would enrich scientists understanding of its anticancer mechanism and facilitate the development of MC-based anticancer products.

Therefore, we investigated the effects of MC on the viability, proliferation, and apoptosis of liver cancer cells *in vitro* and *in vivo*. Gene expression in liver cancer cells was analyzed by using RNA sequencing. In addition, the potential anticancer mechanisms of MC were extensively explored. This study provides insight into MC's use against liver cancer and helps with development of therapy for liver cancer.

Materials and methods

Reagents and drugs

Magnesium cantharidate (MC) (purity ≥98%) was independently researched and developed by a research group and it is covered by Chinese invention patent (ZL201110149288.5). Human liver cancer cell lines Huh-7 and SK-Hep-1 were obtained from Wuhan Lingsi Biotechnology Co., Ltd. (Wuhan, China). Cell Counting Kit-8 (CCK-8) assay kit (item no. C008-3) was purchased from Seven Seas Biomedical Technology Co., Ltd. Mouse anti-Ki-67 antibody (item no. GB12-1141), horseradish peroxidase (HRP)-labeled goat anti-mouse secondary antibodies (item no. GB23301), and HRP-labeled goat antirabbit secondary antibodies (item no. GB23303) were obtained from Wuhan Servicebio Technology Co., Ltd. (Wuhan, China). Rabbit anti-RACK1 antibody (item no. DF7014) and rabbit anti-glyceraldehyde-3-phosphate dehydrogenase (GAPDH) (item no. AF7021) were obtained from Affinity Biosciences (Cincinnati, OH, USA). The EdU Detection Kit (item no. C0071S) was purchased from Jiangsu Biyuntian Biotechnology Co., Ltd. (Changzhou, China), and the SYBR Green PCR kit (item no. AQ131) was purchased from TransGen Biotechnology Co., Ltd. (Changzhou, China).

Analysis of RACK1 expression and correlation

The expression level of RACK1 in liver cancer tissues and its correlation with clinicopatho-

logic data were assessed by using The Cancer Genome Atlas (TCGA) online analysis database (NCBI, Bethesda, MD, USA). The expression of RACK1 in liver cancer tissues was analyzed using the Human Protein Atlas (HPA).

Molecular docking

RACK1 structures were obtained from the Research Collaboratory for Structural Bioinformatics Protein Data Bank database (San Diego, CA, USA). Indraw 6.2.1.0 (Accelrys, San Diego, CA, USA) was used to construct the MC structure. AutoDock (Scripps Research Institute, La Jolla, CA, USA) was used to analyze the docking active site, binding energy, and root-mean-square deviation. PyMol (Schrödinger, LLC, New York, NY, USA) was used to analyze the docking results.

Construction of cell lines overexpressing RACK1

RACK1 cDNA was synthesized using the sequence of the human RACK1 gene retrieved from NCBI (accession number NM_006098.5). DNA was inserted into the pCDH-CMV-MCS-EF1-copGFP-T2A-Puro vector (the third generation of the slow virus carrier system) to generate the RACK1 overexpression vector (pCDH-RACK1). The pCDH-RACK1 and helper plasmids pSPAX2 and pMD2.G were cotransfected into 293T cells for lentiviral packaging. The viral supernatant was harvested by ultracentrifugation (12000 rpm for 10 min). The SK-Hep-1 cell line stably overexpressing RACK1 was then established by using a lentivirus. The multiplicity of infections was 20.

Grouping of cells

The basal media for the Huh-7 and SK-Hep-1 cells were DMEM and minimum essential medium, respectively. The complete medium included basal medium supplemented with 10% fetal bovine serum and 1% penicillin-streptomycin. The cells were cultured at 37°C with 5% carbon dioxide (CO_2) in an incubator. Cells were seeded in a six-well plate at 5×10^5/well and randomly divided into the following groups: control, MC, RACK1 overexpression (OV-RACK1), and RACK1 overexpression +MC (OV-RACK1+MC). MC was administered at a concentration of 1.13 μmol/L. The MC treatment dose was based on the dose used in a previous study [21-23].

CCK-8 assay

Cells were seeded into 96-well plates at a concentration of 5×10^4 cells per well in a volume of 100 μL. Cells were grouped and treated, based on the "grouping of cells". CCK-8 solution (10 μL) was added to each well. After 1 h of incubation, the absorbance was recorded at 450 nm using a spectrophotometer.

EdU assay

The cells were seeded in 24-well plates at a density of 2×10^5 cells/well. Cells were grouped and treated, based on the "grouping of cells". Cell proliferation was assessed using an EdU assay kit, based on the manufacturer's instructions.

Flow cytometry detection

A cell suspension with a concentration of 2×10^5 cells/mL was prepared and evenly distributed into 6-well plates at 2 mL per well. Cells were grouped and treated, based on the "grouping of cells". Cell apoptosis was assessed using flow cytometry with the Annexin V FITC Apoptosis Detection Kit I (BD Biosciences).

Quantitative real-time PCR

TRIzol was used to extract total RNA from the cell samples, and cDNA was synthesized by using a reverse transcription kit. The reaction procedure for quantitative real-time PCR (qRT-PCR) was as follows: 94°C for 30 s, followed by 40 PCR cycles at 94°C for 5 s, 61°C for 35 s, 95°C for 10 s, 65°C for 60 s, and 97°C for 1 s. **Table 1** shows the sequences utilized in this study.

Western blotting

RIPA was used to collect total proteins, and the protein concentration was determined by BCA. SDS-PAGE was used to separate total proteins, which were then semi-dry electrotransferred to a nitrocellulose membrane. RACK1 antibody (1:1000) and GAPDH antibody (1:10000) was added and incubated overnight at 4°C. The membrane was then incubated with HRP-labeled sheep antirabbit secondary antibody for 90 min at 37°C, followed by three washes with Tris-buffered saline with Tween 20 (TBST) for 5 min each. The membranes were then immersed

Table 1. Primer sequences used in qRT-PCR

Primer	Accession number	Sequence (5'-3')
humo-ITPR3-F	NM_002224.4	TCAACCTGTTTATGCAGTTTCGG
humo-ITPR3-R		GCAGCTTGCCCTTGTACTCGTC
humo-FGF19-F	NM_005117.3	GGGCCACTTGGAATCTGACA
humo-FGF19-R		CAAAGCTGGGACTCCTCACG
humo-STIM1-F	NM_001277961.3	GACAGGGACTGTGCTGAAGATGAC
humo-STIM1-R		TCCTTGGAGTAACGGTTCTGGATAT
humo-Vimentin-F	NM_003380.5	GAAGGAGGAAATGGCTCGTCAC
humo-Vimentin-R		GAGTGGGTATCAACCAGAGGGAGT
humo-E-cadherin-F	NM_001317184.2	AGAACGCATTGCCACATACAC
humo-E-cadherin-R		AAGAGCACCTTCCATGACAGAC
humo-N-cadherin-F	NM_001308176.2	AACGCCAGGCCAAACAACTT
humo-N-cadherin-R		ATTCGTCGGATTCCCACAGG
humo-CTBP1-AS2-F	NR_033339.1	CGGGCAACCGTTCTGATTC
humo-CTBP1-AS2-R		CCCTTGTCTTGAGCGTGATACTG
humo-CFAP298-TCP10L-F	NR_146638.2	CCTGCTAGTATCTCCGCAACCT
humo-CFAP298-TCP10L-R		ACTGGCTTACGGGACCTATGAA
humo-HSPE1-MOB4-F	NM_001202485.2	GATGGTGCTGCATGTCTTCTG
humo-HSPE1-MOB4-R		CGGCATACTGATCCTAGTTTCG
humo-RACK1-F	NM_006098.5	GCCATACCAAGGATGTGCTGAGTG
humo- RACK1-R		CACAGGAGACGATGATAGGGTTGC
humo-GAPDH-F	NM_001256799.3	CAAATTCCATGGCACCGTCA
humo-GAPDH-R		GACTCCACGACGTACTCAGC

qRT-PCR, quantitative reverse transcription polymerase chain reaction.

in a luminescent solution for 2 min and imaged using the ECL detection system.

RNA sequencing

Eukaryotic mRNA was sequenced by Wuhan Lingsi Biotechnology Co., Ltd. (Wuhan, China). Differential expression analysis was conducted using DESeq2 (Harvard University, Boston, MA, USA). Multiple hypothesis testing corrections for *P*-values were implemented by controlling the false discovery rate (FDR). Differentially expressed genes (DEGs) were defined as genes with a |FoldChange| ≥2 and *P*-value ≤0.05. ClusterProfiler was utilized for Gene Ontology (GO) and Kyoto Encyclopedia of Genes and Genomes (KEGG) enrichment analysis. Gene Set Enrichment Analysis (GSEA) was performed using ClusterProfiler (version 3.8.1) with FDR-adjusted P<0.05 as the threshold for filtering significant enrichment results. Protein-protein interactions (PPI) were analyzed using String with database version 11.5 (University of Copenhagen. Copenhagen, Denmark), and the R package STRINGdb (version 2.8.4; University of Copenhagen).

The RNA-seq data used in this study was deposited in the Science Data Bank under DOI 10.57760/sciencedb.11456. The online version contains the RNA-seq data, available at https://www.scidb.cn/en/s/yuU3ui.

Animal experiments

Male BALB/c nude mice, aged 4-5 weeks (weight, 12-20 g), were obtained from Ziyuan Laboratory Animal Science and Technology Co., Ltd. (Hangzhou, China). Mouse were fed in a SPF animal laboratory at the Laboratory Animal Center of Zunyi Medical University (Zunyi, China) under a 12-h/12-h light/dark cycle. During the entire study period, mice were provided *ad libitum* with food and water and kept in a controlled environment with a stable temperature of 25°C. After a 7-day adaptation period, the mice were randomly divided into: control, MC, OV-RACK1, and OV-RACK1+MC, with six mice in each group. The SK-Hep-1 cell line, which stably overexpressed RACK1, was used to construct a nude mouse subcutaneous transplantation tumor model. Approximately 1×10^6 SK-

Hep-1 cells (100 μL) were subcutaneously injected into the midposterior area of the right axilla of mice. When the average tumor volume reached approximately 50-70 mm^3, the control group and OV-RACK1 group were injected with the same volume of sterile saline, whereas the MC group was administered with a mass concentration of 120 μg/mL for 18 consecutive days. The MC dose was based on the dose used in our previous study [24]. Every 2 days after drug administration, the long (a) and short (b) diameters of the tumors were measured with Vernier calipers to calculate the tumor volume by using the formula: volume (v) = $a \times b^2/2$. Twenty-four hours after the last drug administration, 1% pentobarbital sodium (50 mg/kg) was injected intraperitoneally, and all nude mice were euthanized by cervical dislocation. Tumor tissue samples were collected, cleaned with precooled physiologic saline, and weighed after the filter paper had dried and absorbed. All animal experimental procedures were approved by the Institutional Animal Care and Use Committee of Zunyi Medical University (approval no.: ZMU21-2107-016).

Ki-67 staining

Nude mouse tumor tissues were dehydrated, embedded, and sectioned after fixation with 4% paraformaldehyde. Antigen repair was performed using 0.01M sodium citrate buffer solution. A 3% hydrogen peroxide solution was used to block endogenous peroxidase, followed by closure with 10% goat serum. Mouse Ki-67 primary antibody was added dropwise and incubated overnight at 4°C. An anti-mouse secondary antibody was applied, and 2,3-diaminobenzidine was used for color development. Samples were stained with hematoxylin staining, followed by sealing with a neutral resin.

Statistical methods

All data were expressed as mean ± standard deviation (SD). GraphPad Prism (version 9.5.1; DotMatics, Hertfordshire, UK) was used to analyze the data and produce graphs. The unpaired Student's t-test was used to compare two groups. One-way analysis of variance (ANOVA) was used to compare the differences between multiple groups, followed by Tukey's multiple comparison test. A value of $P<0.05$ indicated a significant difference.

Results

RACK1 was significantly associated with poor prognosis in HCC

TCGA analysis revealed a substantial upregulation of RACK1 in liver cancer cells, compared to normal liver cells (all: P<0.01). It also revealed a notable association with TP53 mutation status, histological subtype, tumor grade, individual cancer stage, and survival in liver cancer (all: P<0.01) (**Figure 2A-F**). RACK1 expression in liver tissues was further explored by using the HPA database. We confirmed significant overexpression of RACK1 in liver cancer cells (HPA: https://www.proteinatlas.org/ENSG00000204628-RACK1/pathology/liver+cancer), compared with normal liver cells (HPA: https://www.proteinatlas.org/ENSG00000204628-RACK1/tissue/liver) (**Figure 2G-I**). These findings collectively indicated that, in the context of liver cancer, RACK1 exhibited a pronounced elevation in expression and was significantly correlated with the development and progression of liver cancer.

MC inhibited RACK1 expression

First, we used molecular docking to assess the docking accuracy of RACK1 with MC. The molecular docking results indicated that the minimum binding energy of RACK1 was -5.8 kcal/mol, which is lower than -5.0 kcal/mol, suggesting a strong interaction between MC and RACK1 (**Figure 3A**). To assess the effect of MC on RACK1 expression in liver cancer cells, we examined RACK1 expression using qRT-PCR and western blotting. Our results demonstrated that MC treatment significantly inhibited RACK1 expression in normal Huh-7 and SK-Hep-1 cells (all: P<0.01). In addition, MC treatment significantly inhibited RACK1 expression in RACK1-overexpressing Huh-7 and SK-Hep-1 cells (all: P<0.01) (**Figure 3B-D**). These findings collectively highlighted the ability of MC to inhibit the expression of RACK1 in Huh-7 and SK-Hep-1 cells.

MC diminished cell viability and proliferation by targeting RACK1

We used CCK8 and EdU assays to evaluate the effects of MC and RACK1 on the viability and proliferation of liver cancer cells, respectively. Our results revealed a noteworthy decrease in

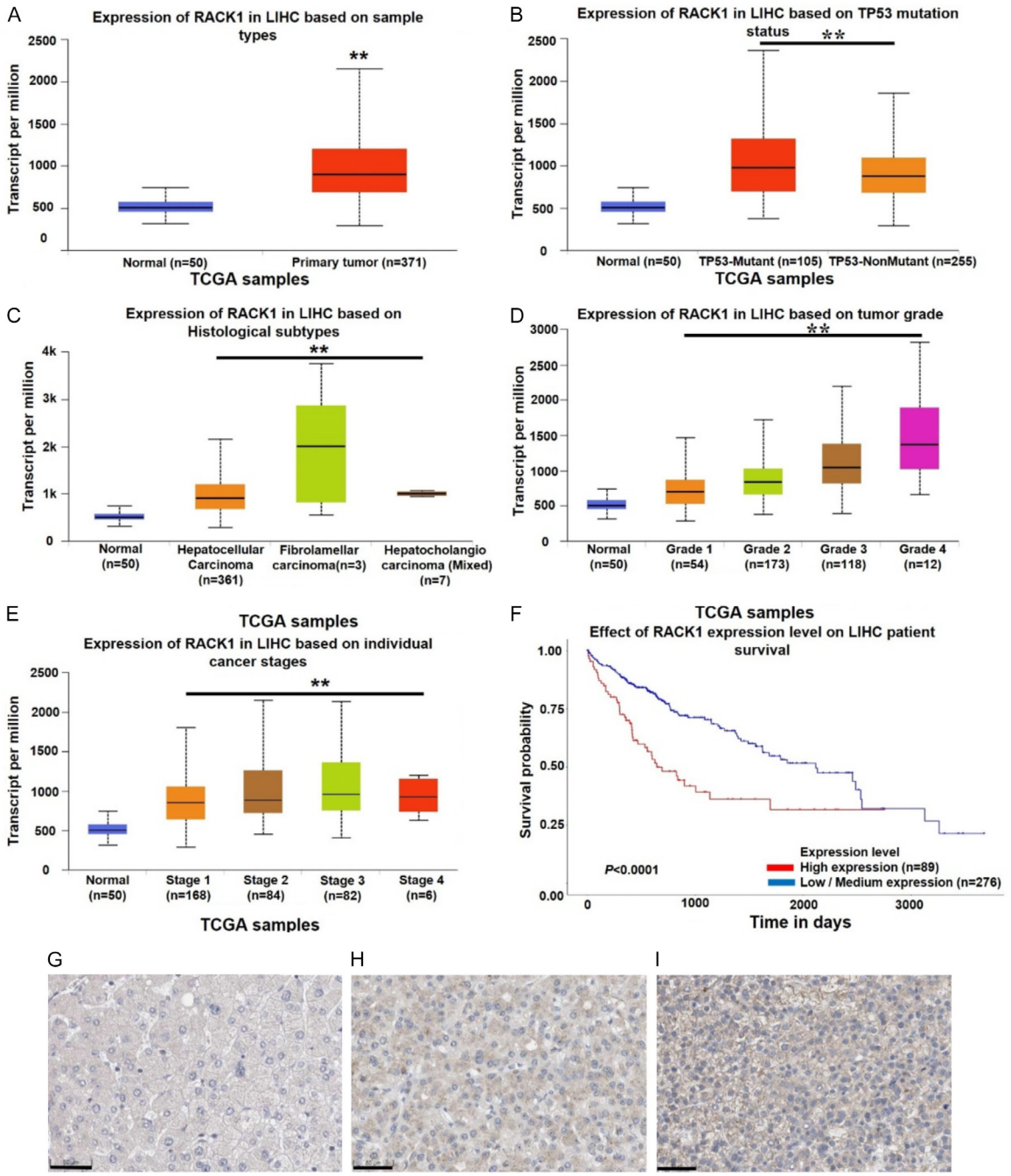

Figure 2. RACK1 was significantly associated with the clinicopathology of liver cancer. A. Expression of RACK1 in liver cancer and normal liver tissues. B. Expression of RACK1 in normal liver tissues and in TP53-mutated and TP53-nonmutated liver cancer tissues. C. Expression of RACK1 in different histological subtypes. D. Expression of RACK1 in different tumor grades. E. Expression of RACK1 in different cancer stages. F. Relationship between RACK1 expression in liver cancer tissues and liver cancer survival curves. G. Immunohistochemistry (IHC) assay was used to assess the expression of RACK1 in human normal liver tissues (n=3) (https://www.proteinatlas.org/ENSG00000204628-RACK1/tissue/liver). H and I. IHC assay was used to assess the expression of RACK1 in human liver cancer tissues (n=11) (https://www.proteinatlas.org/ENSG00000204628-RACK1/tissue/liver). The scale bar indicates 50 μm. **Compared to the normal group (P<0.01).

liver cancer cell viability and proliferation in the MC group, compared with the control group (all: P<0.01). However, the viability and proliferation of liver cancer cells were significantly enhanced

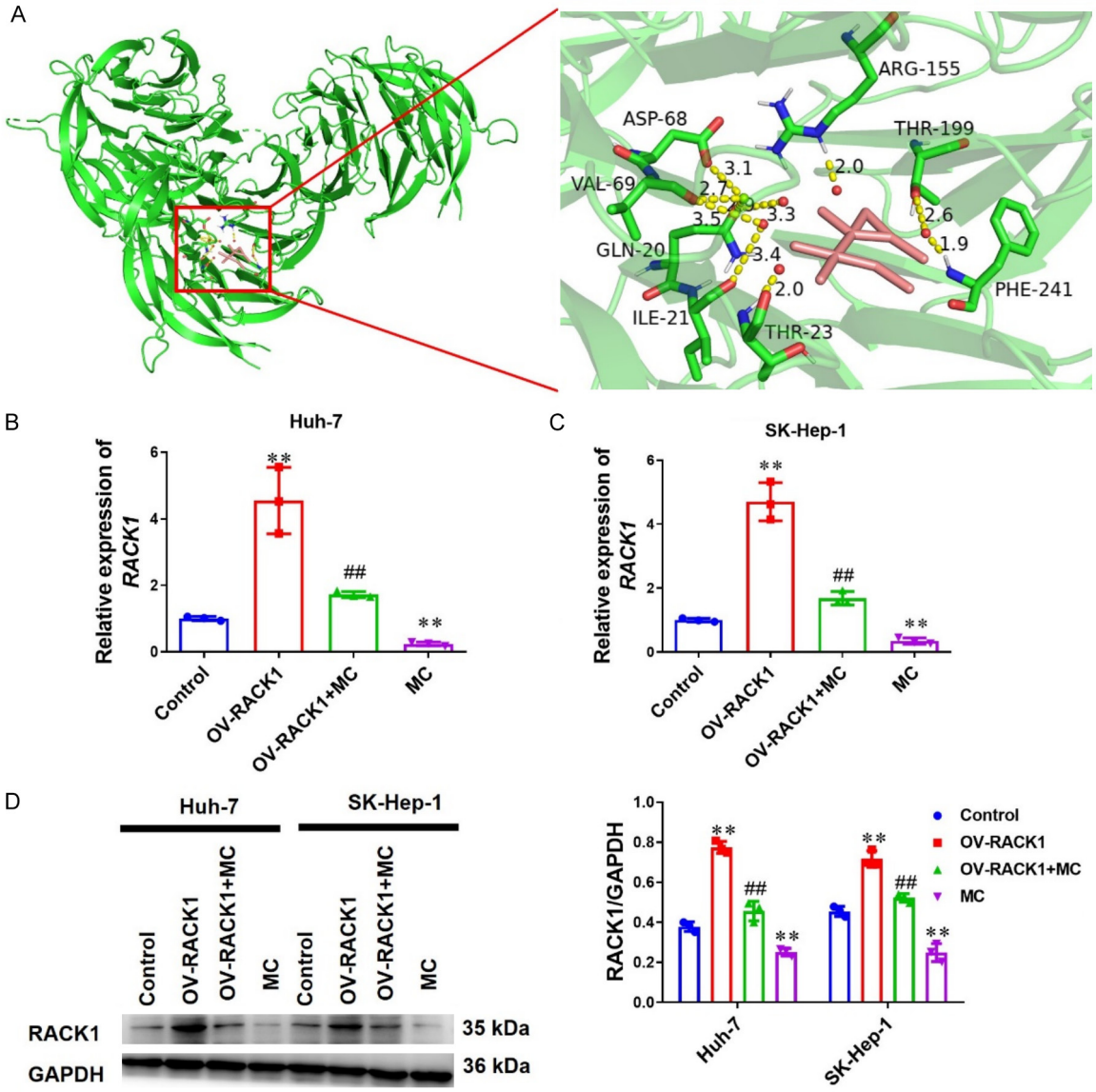

Figure 3. MC inhibited RACK1 expression in liver cancer cells. A. Docking pose between MC and RACK1. This figure illustrates the optimal docking positions of RACK1 for MC. The pink molecule represents MC. The amino acid residues ASP-68 and ARG-155 on RACK1 interact with MC. The yellow dashed lines indicate hydrogen bonds. B. qRT-PCR was performed to detect RACK1 mRNA expression in Huh-7 cells (n=3). C. qRT-PCR was performed to detect RACK1 mRNA expression in SK-Hep-1 cells (n=3). D. Western blotting was performed to detect RACK1 protein expression in Huh-7 and SK-Hep-1 cells (n=3). **compared to the control group (P<0.01). ##compared to the OV-RACK1 group (P<0.01).

in the OV-RACK1 group (all: P<0.01). An intriguing finding was that, in the OV-RACK1+MC treatment group, liver cancer cell viability and proliferation were markedly diminished, compared to those in the OV-RACK1 group (all: P<0.01) (**Figure 4**). These results indicated that the overexpression of RACK1 substantially elevated the viability and proliferation of liver cancer cells. However, MC significantly inhibited the viability and proliferation of liver cancer cells. Thus, the results suggested that MC inhibits cell proliferation induced by RACK1 overexpression.

MC promoted apoptosis by targeting RACK1

Compared to the control group, the MC group exhibited a significantly higher rate of apoptosis in liver cancer cells (all: P<0.01). The OV-RACK1 group conversely showed a significantly

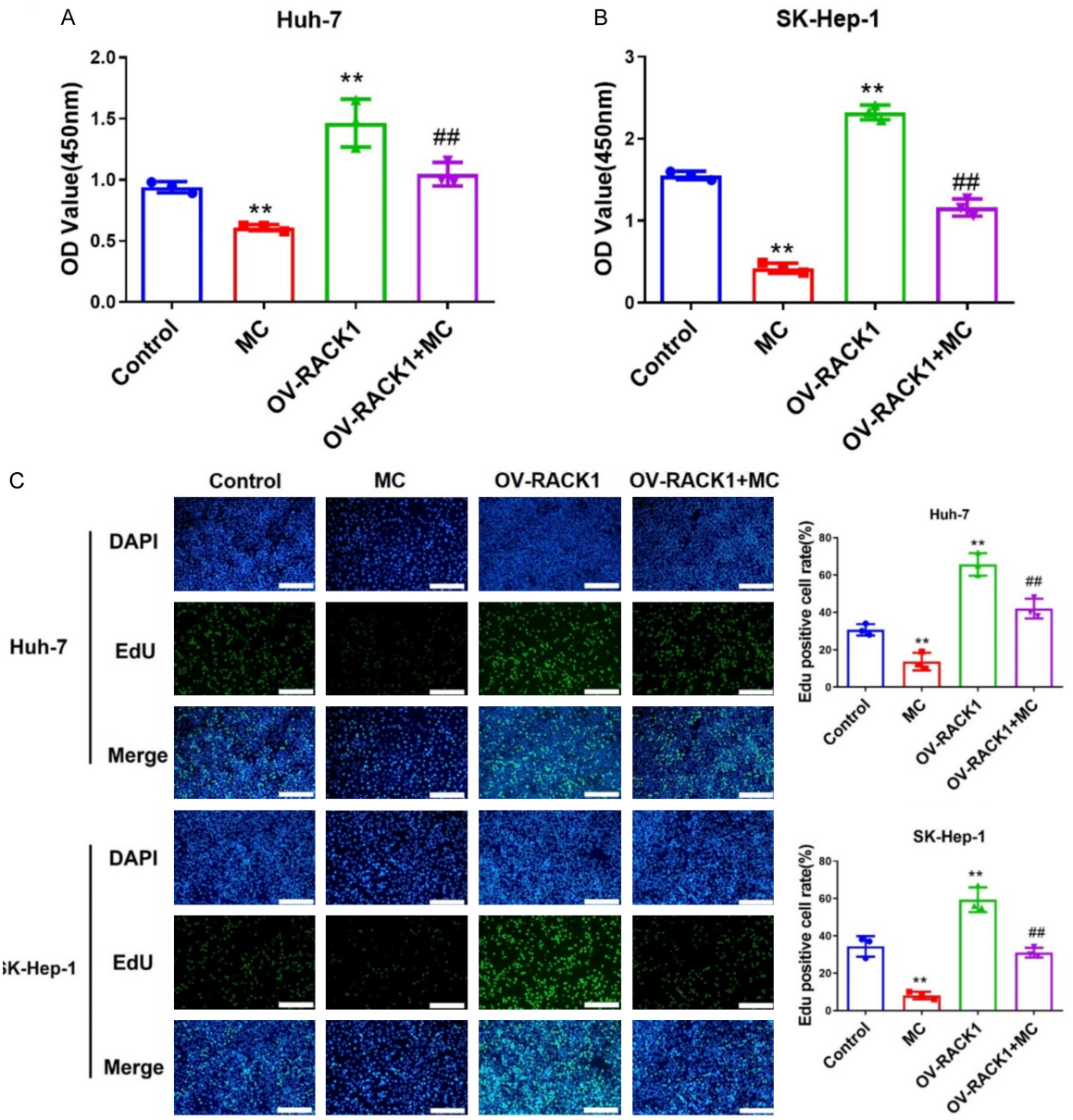

Figure 4. MC diminished viability and proliferation of liver cancer cells. A. The CCK-8 assay was used to detect the viability of Huh-7 cells (n=3). B. CCK-8 assay was used to detect the viability of SK-Hep-1 cells (n=3). C. EdU was used to detect the proliferative ability of Huh-7 and SK-Hep-1 cells (n=3). The scale bar indicates 100 μm. **compared to the control group (P<0.01). ##compared to the OV-RACK1 group (P<0.01).

lower rate of apoptosis in liver cancer cells (all: P<0.01). An interesting finding is that the OV-RACK1+MC group displayed a significantly elevated apoptosis rate in liver cancer cells, compared with the OV-RACK1 group (all: P<0.01) (**Figure 5**). These findings underscore the role of RACK1 in inhibiting apoptosis and the role of MC in promoting apoptosis in liver cancer cells. Thus, these results suggested that MC promotes apoptosis by inhibiting RACK1 overexpression.

MC inhibited tumor growth in vivo

Compared to the control group, the MC group exhibited significantly reduced tumor volume, weight, and Ki-67 expression (all: P<0.01). The OV-RACK1 group conversely showed a significant increase in tumor volume, weight, and Ki-67 expression (all: P<0.01). An intriguing finding was that tumor formation volume, weight, and Ki-67 expression were markedly diminished in the OV-RACK1+MC group, compared to

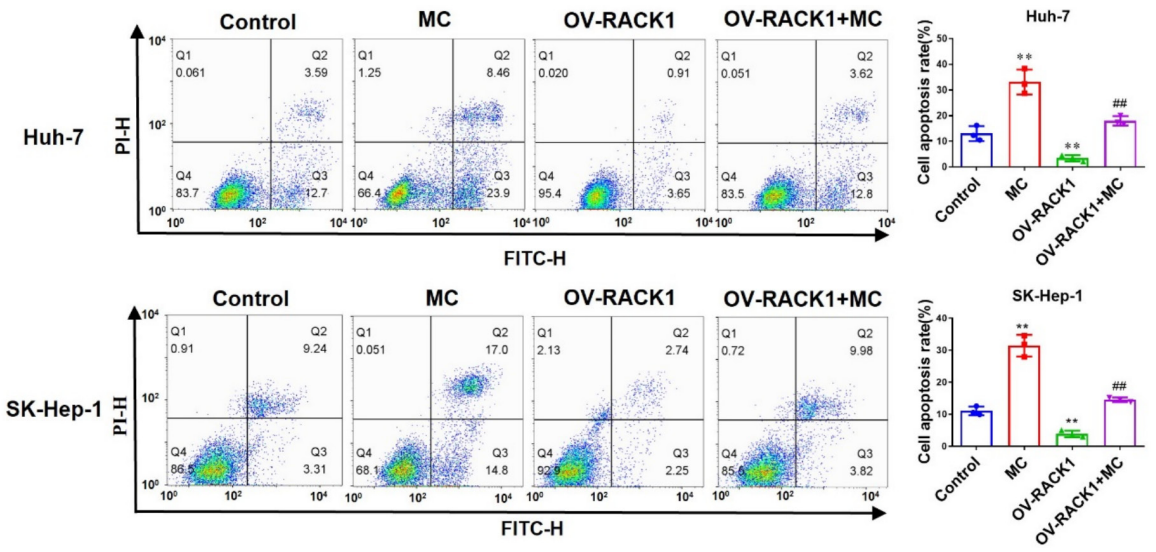

Figure 5. MC promoted apoptosis in liver cancer cells (n=3). **compared to the control group (P<0.01). ##compared to the OV-RACK1 group (P<0.01).

the OV-RACK1 group (all: P<0.01) (**Figure 6**). These outcomes underscore the considerable effect of RACK1 in promoting liver cancer cell proliferation and the potential of MC intervention for mitigating their proliferative capacity.

Screening of DEGs in liver cancer cells after MC intervention

Cluster analysis identified variations in gene expression across distinct treatment groups. The analysis revealed that, in normal SK-Hep-1 cells, MC treatment led to 106 DEGs, comprising 44 downregulated and 62 upregulated genes. Overexpression of RACK1 resulted in 2660 DEGs, including 469 downregulated and 2191 upregulated genes. Of note, in RACK1 SK-Hep-1 cells, MC treatment induced 111 DEGs, which included 26 downregulated and 85 upregulated genes (**Figure 7A-C** and **Table 2**). Furthermore, Venn diagram analysis highlighted CTBP1-AS2, CFAP298-TCP10L, and HSPE1-MOB4 as DEGs shared between the two comparison groups (**Figure 7D**). qRT-PCR results revealed that MC intervention significantly inhibited CTBP1-AS2 and HSPE1-MOB4 expression (all: P< 0.01) and promoted CFAP298-TCP10L expression (all: P<0.01) in RACK1-overexpressing SK-Hep-1 cells (**Figure 7E-G**).

GO/KEGG analysis of DEGs

GO analysis revealed that DEGs under MC treatment were primarily involved in the cellular response to hormonal stimuli, cellular response to calcium ions, and adenosine triphosphate (ATP) hydrolysis activity. DEGs induced by RACK1 overexpression were primarily related to cell division, DNA replication, cellular response to DNA damage, G1/S transition of the mitotic cell cycle, and DNA helicase activity. In SK-Hep-1 cells with RACK1 overexpression, the primary focus of DEGs under MC treatment was on the regulation of cytosolic calcium ion concentration and cell-cell adhesion through plasma membrane adhesion (**Figure 8A-C** and **Table 3**). Furthermore, KEGG analysis results revealed that DEGs under MC treatment were primarily enriched in the NF-κB signaling pathway and Toll-like receptor signaling pathway in SK-Hep-1 cells. The overexpression of RACK1 induced DEGs that were predominantly associated with the cell cycle. In SK-Hep-1 cells overexpressing RACK1, DEGs under MC treatment were primarily enriched in the vascular endothelial growth factor and MAPK signaling pathways (**Figure 8D-F** and **Table 4**). In summary, RACK1 overexpression influenced genes linked to cell differentiation, DNA replication, and damage repair, and promoted cell proliferation, whereas MC treatment primarily elevated the expression of genes related to calcium channels, cellular metabolism, protein binding, and overall cellular metabolism.

GSEA analysis of DEGs

GSEA/GO results showed that MC treatment increased the expression of genes associated

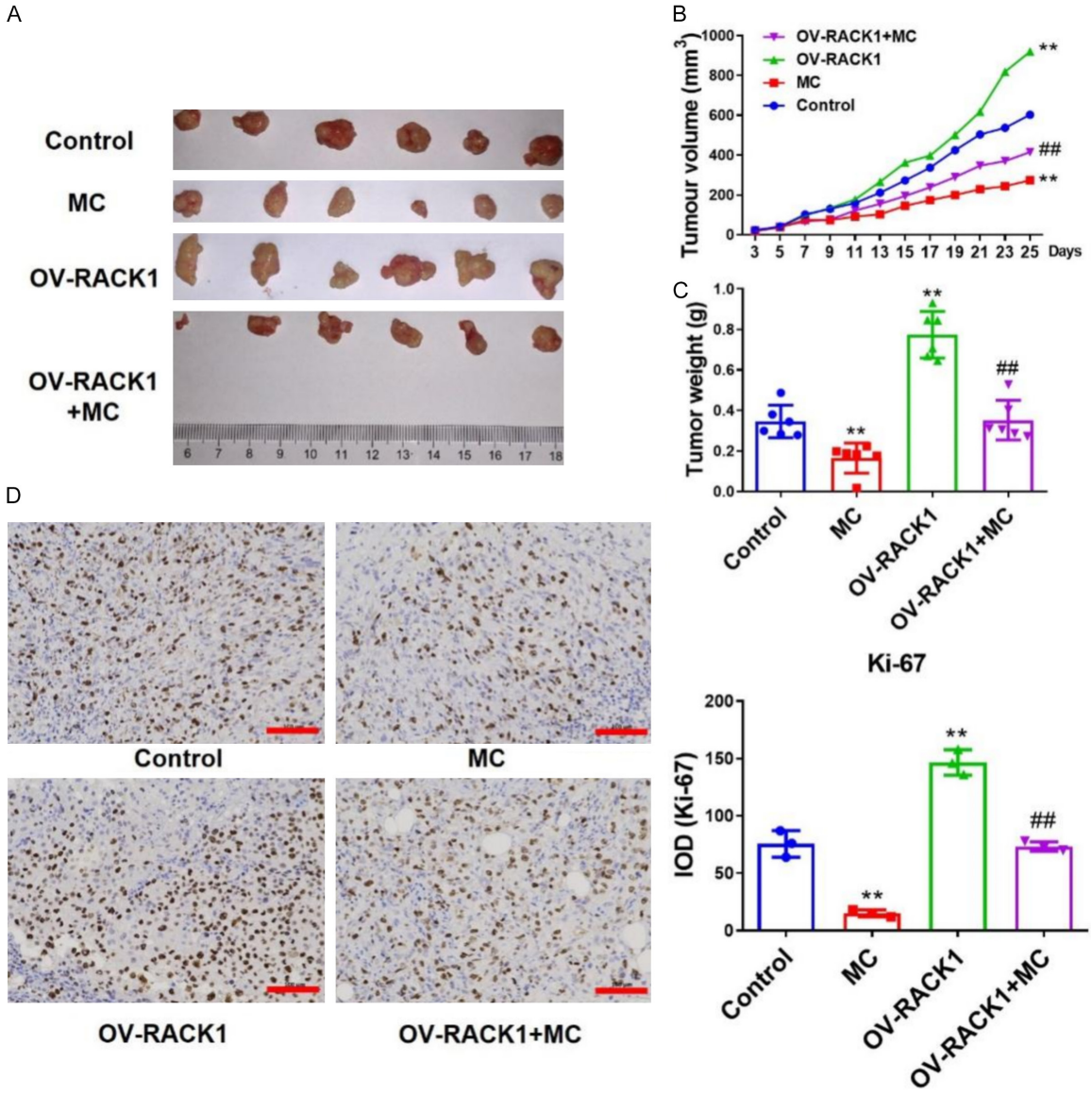

Figure 6. MC inhibited tumor growth *in vivo*. A. *In vivo* tumor images of nude mice (n=6). B. *In vivo* tumor growth curves of nude mice (n=6). C. *In vivo* tumor weights in nude mice (n=6). D. Ki-67 expression was detected via immunohistochemistry (IHC) (n=3). The scale bar indicates 100 μm. **compared to the control group (P<0.01). ##compared to the OV-RACK1 group (P<0.01).

with the proteasome core complex, phosphatidylinositol 3-kinase binding, iron ion transport, and chloride transport in SK-Hep-1 cells. The overexpression of RACK1 increased the expression of genes related to DNA replication, cell division, the G1/S transition of the mitotic cell cycle, and DNA repair. In SK-Hep-1 cells overexpressing RACK1, MC treatment increased the expression of genes involved in calcium-dependent cell-cell adhesion by plasma membrane cell adhesion molecules and the regulation of I-κB kinase/NF-κB signaling (**Figure 9A-C** and **Table 5**). GSEA/KEGG results showed that MC treatment upregulated genes associated with nucleotide excision repair and the proteasome, whereas RACK1 overexpression upregulated genes linked to the cell cycle, DNA replication, and nucleotide excision repair. MC treatment increased the expression of genes associated with ferroptosis, cell adhesion molecules, ribosomes, and the Toll-like receptor signaling pathway in RACK1 SK-Hep-1 cells (**Figure 9D-F** and **Table 6**). In summary, the GSEA results revealed that the overexpression of RACK1 pre-

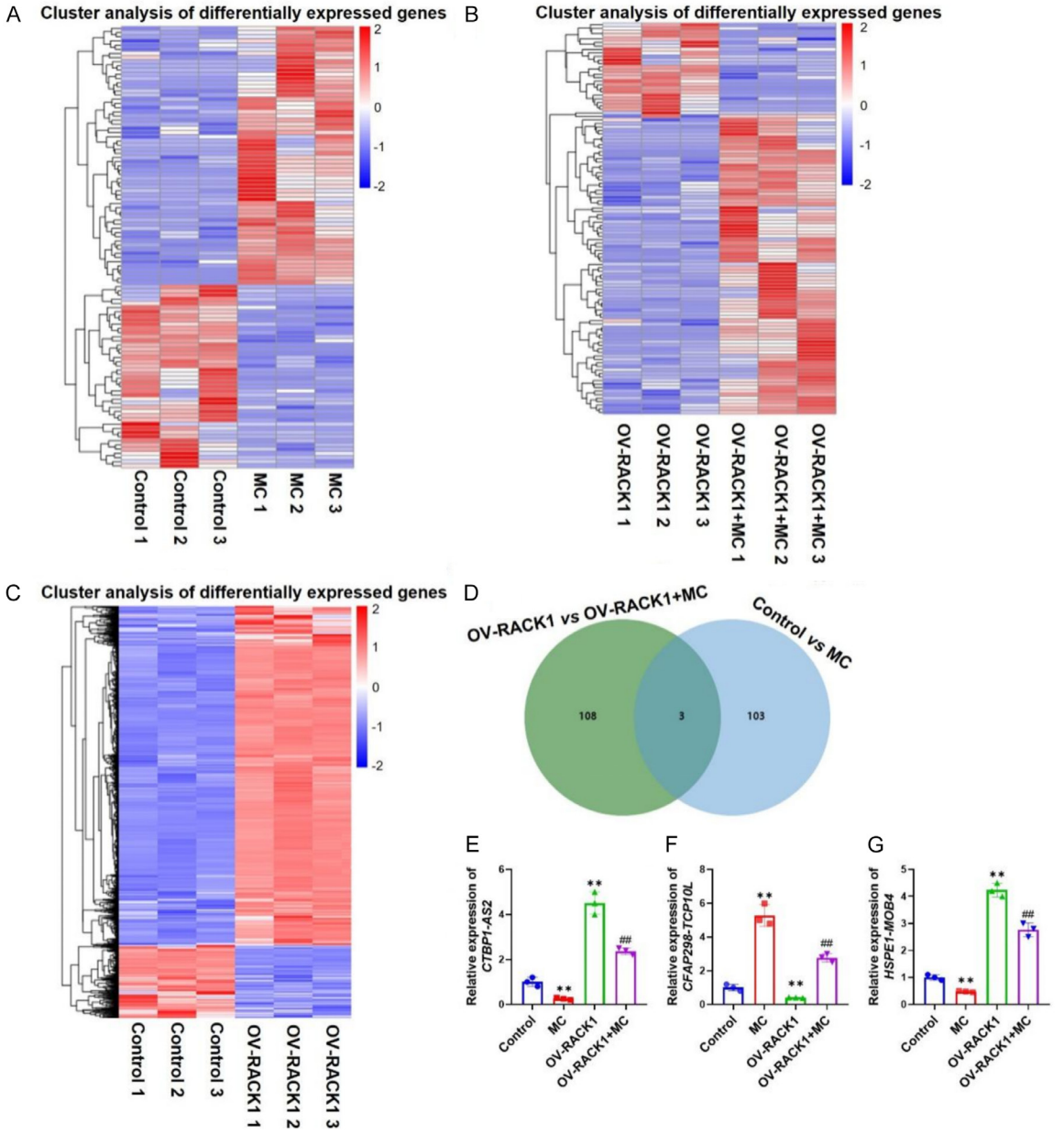

Figure 7. Differential expression gene analysis between different SK-Hep-1 cell treatment groups. (A) SK-Hep-1 control group *vs.* MC-treated group. (B) RACK1 overexpression group *vs.* RACK1 overexpression+MC group. (C) SK-Hep-1 control group *vs.* RACK1 overexpression group. (D) Venn diagram of differential expression genes in different treatment groups. (E-G) qRT-PCR was used to detect CTBP1-AS2 (E), CFAP298-TCP10L (F), and HSPE1-MOB4 (G) mRNA expression in SK-Hep-1 cells (n=3). *vs.*: versus. **compared to the control group ($P<0.01$). $^{\#\#}$compared to the OV-RACK1 group ($P<0.01$).

dominantly influenced genes related to cell differentiation, cell cycle, and DNA replication, whereas MC treatment primarily affected genes related to cell metabolism, ion channels, and nucleotide repair. The overexpression of RACK1 enhanced cell proliferation, whereas MC treatment promoted cellular metabolism and related functions.

Expression analysis of calcium ion transport, ion channels, and cell adhesion genes

Bioinformatic analysis suggested that MC inhibited liver cancer proliferation and promoted apoptosis by regulating calcium ion transport, ion channels, and cell adhesion pathways. Therefore, calcium ion transport and ion channel pa-

Table 2. Up/down-regulation of the top three differential genes between different SK-Hep-1 cell treatment groups

Group	Up/Down	GeneID	Log_2FoldChange	Pval	Padj
Control *vs* MC	Up	TAGLN	1.03	1.14E-28	0.00
		CALD1	1.17	6.77E-22	0.00
		C21orf59-TCP10L	1.79	3.33E-11	0.00
	Down	FOS	-1.24	5.85E-72	0.00
		FOSB	-1.05	3.41E-28	0.00
		PHOSPHO2-KLHL23	-7.40	0.00	0.03
OV-RACK1 *vs* OV-RACK1+MC	Up	SSPO	1.08	4.77E-06	0.00
		LOC105377650	1.06	2.2E-05	0.00
		PGBD3	1.49	6.12E-05	0.00
	Down	GABPB1-AS1	-2.11	8.54E-18	0.00
		CTBP1-AS2	-1.69	1.76E-06	0.00
		GPR75-ASB3	-2.06	0.00	0.02
Control *vs* OV-RACK1	Up	IPO7	1.63	4.2E-294	0.00
		DDX21	1.73	2.1E-288	0.00
		TNPO1	1.58	2.4E-288	0.00
	Down	IFITM1	-1.91	1.2E-288	0.00
		BATF2	-2.13	8.6E-280	0.00
		OAS2	-1.47	2E-269	0.00

MC, magnesium cantharidate; OV-RACK1, overexpression of receptor for activated C kinase 1.

thway genes, such as inositol 1,4,5-trisphosphate receptor 3 (ITPR3), fibroblast growth factor (FGF)-19, stromal interaction molecule 1 (STIM1), and cell adhesion pathway genes, such as vimentin, E-cadherin, and N-cadherin, were detected in SK-Hep-1 cells using qRT-PCR. The qRT-PCR results revealed that the overexpression of RACK1 significantly facilitated ITPR3, FGF19, STIM1, vimentin and N-cadherin expression and inhibited E-cadherin expression, whereas MC reversed the effects of RACK1 overexpression in SK-Hep-1 cells. Moreover, MC intervention inhibited ITPR3, FGF19, STIM1, vimentin and N-cadherin expression, and promoted E-cadherin expression in SK-Hep-1 cells (**Figure 10**). These findings provided evidence that MC inhibited liver cancer cell proliferation and promoted apoptosis by regulating calcium ion transport, ion channels, and cell adhesion pathways.

PPI analysis of DEGs

PPI analysis revealed that MC treatment resulted in the interaction of 65 proteins, forming 11 network interactions in the SK-Hep-1 cells. In particular, FBJ murine osteosarcoma viral oncogene homolog (FOS) interacts closely with FBJ murine osteosarcoma viral oncogene homolog B (FOSB) and CCL4 in these networks. RACK1 overexpression resulted in the interaction of 100 proteins, forming 305 interaction networks. Interactions included CDC6 with ORC6, MSH2 with MSH6, FOSB with JUN, and DZW10 with RINT1. In SK-Hep-1 cells overexpressing RACK1, MC treatment induced interactions among 51 proteins, forming five interaction networks. Of note, CDH22 exhibited close interactions with CDH26, and NLRC4 with TLR5 within these networks (**Figure 11**). In summary, RACK1 overexpression promoted protein interactions associated with cell proliferation, whereas MC treatment increased interactions among proteins related to metabolism.

Discussion

RACK1 shuttles to different subcellular units, mediates PPI, and is positively associated with the progression of esophageal, hepatocellular, ovarian, and breast cancers [25]. Relevant studies have revealed that RACK1 expression is positively associated with vascular cancer embolism, tumor differentiation, TNM stage, lymph node metastasis, and liver cancer metastasis. RACK1 is markedly overexpressed in HCC cells, compared with adjacent noncancerous tissues. Moreover, patients exhibiting elevated RACK1

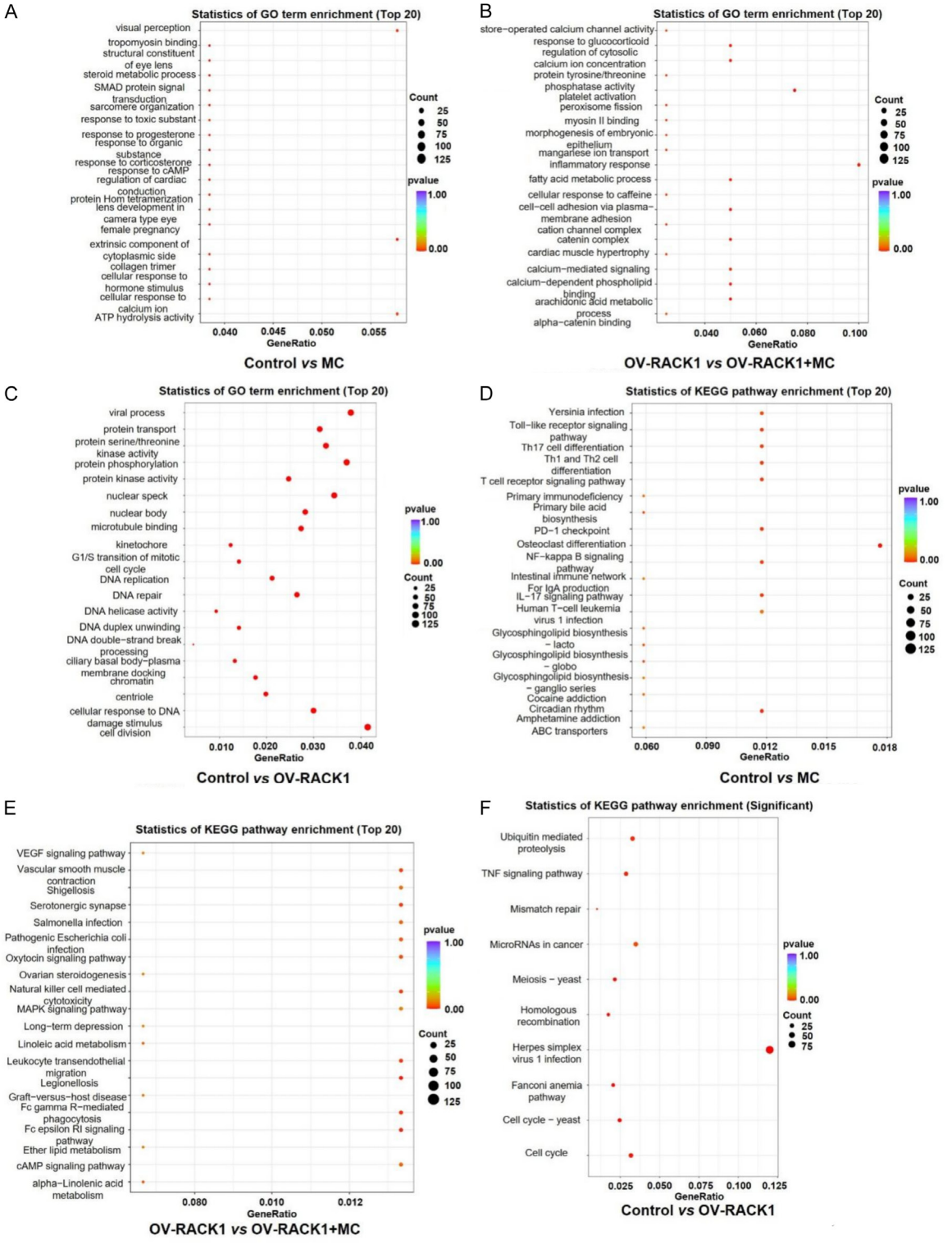

Figure 8. GO and KEGG enrichment analysis of the different SK-Hep-1 cell treatment groups. A. SK-Hep-1 control *vs.* MC-treated group in the GO analysis. B. RACK1 overexpression group *vs.* RACK1 overexpression +MC group in the GO analysis. C. SK-Hep-1 control *vs.* RACK1 overexpression group in the GO analysis. D. SK-Hep-1 control *vs.* MC-treated group in the KEGG analysis. E. RACK1 overexpression group *vs.* the RACK1 overexpression +MC group in the KEGG analysis. F. SK-Hep-1 control group *vs.* RACK1 overexpression group in the KEGG analysis. *vs.*: versus.

Table 3. GO enrichment analysis related to cell proliferation, as well as apoptosis between different SK-Hep-1 cell treatment groups

Group	ID	Description	Pval	Padj
Control *vs.* MC	GO:0005523	Tropomyosin binding	0.00	0.15
	GO:0071277	Cellular response to calcium ion	0.02	0.18
	GO:0016887	ATP hydrolysis activity	0.02	0.19
OV-RACK1 *vs.* OV-RACK1+MC	GO:0015279	Store-operated calcium channel activity	0.02	0.16
	GO:0051480	Regulation of cytosolic calcium ion concentration	0.00	0.16
	GO:0098742	Cell-cell adhesion via plasma membrane adhesion	0.00	0.16
Control *vs.* OV-RACK1	GO:0000082	G1/S transition of mitotic cell cycle	1.81E-08	6.08E-06
	GO:0006260	DNA replication	1.20E-14	2.22E-11
	GO:0003678	DNA helicase activity	8.22E-08	2.33E-05

MC, magnesium cantharidate; OV-RACK1, overexpression of receptor for activated C kinase 1.

Table 4. KEGG enrichment analysis related to cell proliferation, as well as apoptosis between different SK-Hep-1 cell treatment groups

Group	ID	Description	Pval	Padj
Control *vs.* MC	map04620	Toll-like receptor signaling pathway	0.02	0.16
	map04064	NF-kappa B signaling pathway	0.02	0.16
	map04660	T cell receptor signaling pathway	0.02	0.16
OV-RACK1 *vs.* OV-RACK1+MC	map04370	VEGF signaling pathway	0.10	0.29
	map04010	MAPK signaling pathway	0.10	0.29
	map04024	cAMP signaling pathway	0.06	0.29
Control *vs.* OV-RACK1	map04110	Cell cycle	7.28E-05	0.00
	map03430	Mismatch repair	0.00	0.00
	map03440	Homologous recombination	2.56E-06	0.00

KEGG, Kyoto Encyclopedia of Genes and Genomes; Pval, *P* value; Padj, adjusted *P* value; MC, magnesium cantharidate; OV-RACK1, overexpression of receptor for activated C kinase 1; VEGF, vascular endothelial growth factor; MAPK, mitogen-activated protein kinase; cAMP, cyclic adenosine monophosphate.

levels have significantly reduced overall survival rates, compared to patients with lower RACK1 expression [13, 26]. Our results revealed that the expression level of RACK1 was significantly correlated with the clinicopathologic characteristics of liver cancer such as tissue typing, survival, staging, and TP53 mutations, which suggested that RACK1 may predict survival and recurrence in patients with liver cancer.

Wu et al. [27] demonstrated that RACK1 promotes invasion and lymph node metastasis through its interaction with galactose lectin-1 in cervical cancer. Moreover, Wu et al. [28] found that RACK1 could promote proliferation by increasing β-catenin stability and activating the classical WNT signaling pathway. Furthermore, Chen et al. [29] identified isobutyric acid as a RACK1 activator that facilitates downstream Akt and FAK signaling and promotes metastasis in colorectal cancer. By contrast, Huang et al. [30] found that the knockdown of RACK1 inhibited breast cancer cell proliferation and migration and reversed the oncogenic function of ubiquitin-specific protease 41. Zou et al. [15] demonstrated that RACK1 silencing inhibits proliferation and induces apoptosis in MHCC-97-H cells. Consistent with these findings, our study revealed that RACK1 overexpression stimulated cell proliferation and inhibited apoptosis in Huh-7 and SK-Hep-1 cells. Moreover, RACK1 overexpression facilitated the growth of subcutaneously transplanted tumors in vivo. These results collectively underscore the significance of RACK1 as a pivotal gene that drives liver cancer cell proliferation, and suggest it as a target for liver cancer.

Active ingredients derived from herbal sources exhibit diverse biological effects, showcasing their dual capability to effectively impede the proliferation of pathogenic microorganisms while concurrently boosting the body's immune re-

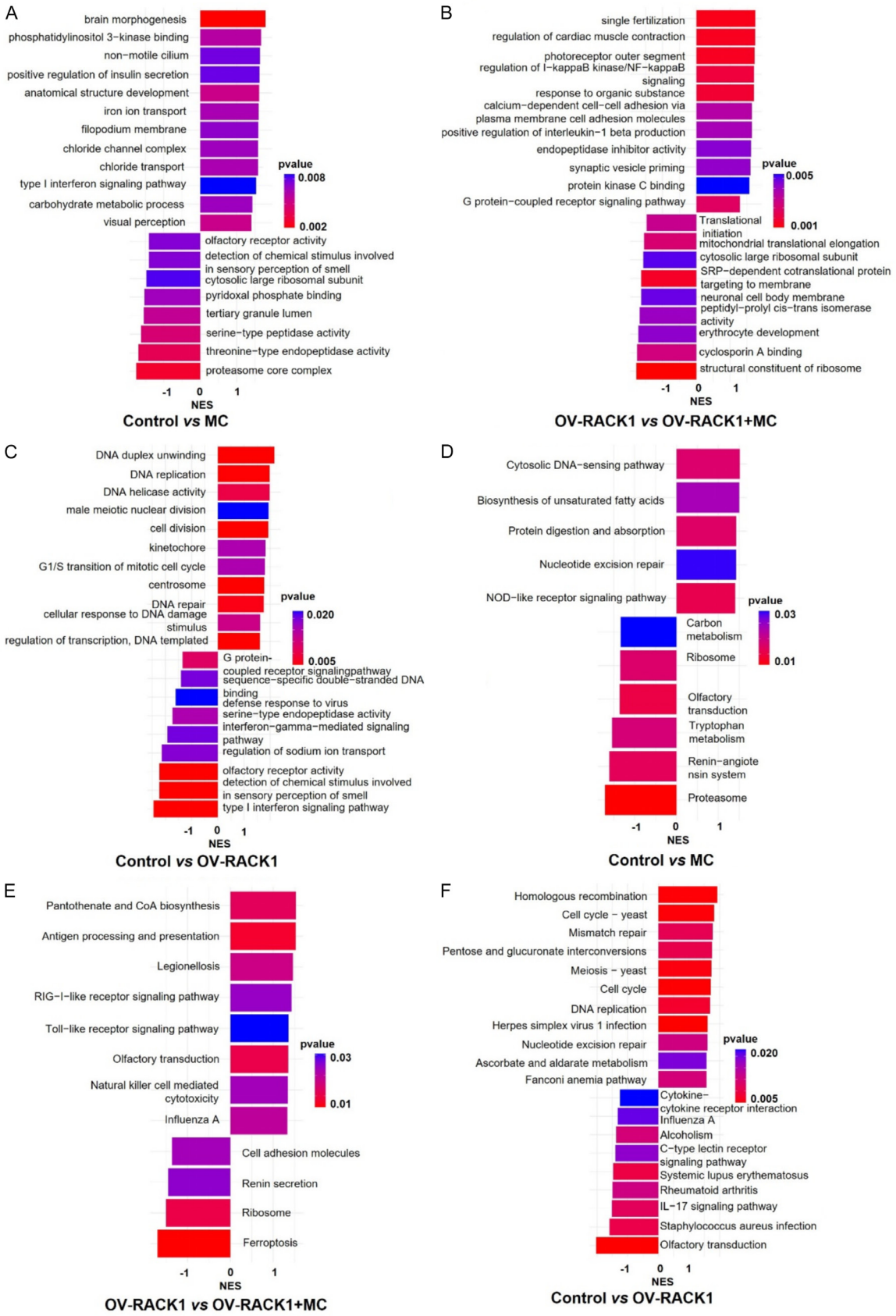
A
brain morphogenesis
phosphatidylinositol 3−kinase binding
non−motile cilium
positive regulation of insulin secretion
anatomical structure development
iron ion transport
filopodium membrane
chloride channel complex
chloride transport
type I interferon signaling pathway
carbohydrate metabolic process
visual perception
olfactory receptor activity
detection of chemical stimulus involved in sensory perception of smell
cytosolic large ribosomal subunit
pyridoxal phosphate binding
tertiary granule lumen
serine−type peptidase activity
threonine−type endopeptidase activity
proteasome core complex
pvalue
0.008
0.002
-1 0 1
NES
Control vs MC
B
single fertilization
regulation of cardiac muscle contraction
photoreceptor outer segment
regulation of I−kappaB kinase/NF−kappaB signaling
response to organic substance
calcium−dependent cell−cell adhesion via plasma membrane cell adhesion molecules
positive regulation of interleukin−1 beta production
endopeptidase inhibitor activity
synaptic vesicle priming
protein kinase C binding
G protein−coupled receptor signaling pathway
Translational initiation
mitochondrial translational elongation
cytosolic large ribosomal subunit
SRP−dependent cotranslational protein targeting to membrane
neuronal cell body membrane
peptidyl−prolyl cis−trans isomerase activity
erythrocyte development
cyclosporin A binding
structural constituent of ribosome
pvalue
0.005
0.001
-1 0 1
NES
OV-RACK1 vs OV-RACK1+MC
C
DNA duplex unwinding
DNA replication
DNA helicase activity
male meiotic nuclear division
cell division
kinetochore
G1/S transition of mitotic cell cycle
centrosome
DNA repair
cellular response to DNA damage stimulus
regulation of transcription, DNA templated
G protein−coupled receptor signaling pathway
sequence−specific double−stranded DNA binding
defense response to virus
serine−type endopeptidase activity
interferon−gamma−mediated signaling pathway
regulation of sodium ion transport
olfactory receptor activity
detection of chemical stimulus involved in sensory perception of smell
type I interferon signaling pathway
pvalue
0.020
0.005
-1 0 1
NES
Control vs OV-RACK1
D
Cytosolic DNA−sensing pathway
Biosynthesis of unsaturated fatty acids
Protein digestion and absorption
Nucleotide excision repair
NOD−like receptor signaling pathway
Carbon metabolism
Ribosome
Olfactory transduction
Tryptophan metabolism
Renin−angiotensin system
Proteasome
pvalue
0.03
0.01
-1 0 1
NES
Control vs MC
E
Pantothenate and CoA biosynthesis
Antigen processing and presentation
Legionellosis
RIG−I−like receptor signaling pathway
Toll−like receptor signaling pathway
Olfactory transduction
Natural killer cell mediated cytotoxicity
Influenza A
Cell adhesion molecules
Renin secretion
Ribosome
Ferroptosis
pvalue
0.03
0.01
-1 0 1
NES
OV-RACK1 vs OV-RACK1+MC
F
Homologous recombination
Cell cycle − yeast
Mismatch repair
Pentose and glucuronate interconversions
Meiosis − yeast
Cell cycle
DNA replication
Herpes simplex virus 1 infection
Nucleotide excision repair
Ascorbate and aldarate metabolism
Fanconi anemia pathway
Cytokine−cytokine receptor interaction
Influenza A
Alcoholism
C−type lectin receptor signaling pathway
Systemic lupus erythematosus
Rheumatoid arthritis
IL−17 signaling pathway
Staphylococcus aureus infection
Olfactory transduction
pvalue
0.020
0.005
-1 0 1
NES
Control vs OV-RACK1

Figure 9. Analysis of GSEA gene enrichment of the different SK-Hep-1 cell treatment groups. A. SK-Hep-1 control *vs.* MC-treated group in the GO analysis. B. RACK1 overexpression group *vs.* RACK1 overexpression + MC group in the GO analysis. C. SK-Hep-1 control group *vs.* RACK1 overexpression group in the GO analysis. D. SK-Hep-1 control group *vs.* MC-treated group in the KEGG analysis. E. RACK1 overexpression group *vs.* RACK1 overexpression + MC group in the KEGG analysis. F. SK-Hep-1 control *vs.* RACK1 overexpression group in the KEGG analysis. *vs.*: versus.

Table 5. Enrichment analysis of GSEA/GO genes associated with cell proliferation, as well as apoptosis between different SK-Hep-1 cell treatment groups

Group	ID	Description	Pval	Padj
Control *vs.* MC	GO:0043548	Phosphatidylinositol 3-kinase binding	0.00	1.00
	GO:0005839	Proteasome core complex	0.00	1.00
	GO:0006826	Iron ion transport	0.00	1.00
OV-RACK1 *vs.* OV-RACK1+MC	GO:0043122	Regulation of I-kappaB kinase/NF-kappaB signaling	0.00	0.33
	GO:0016339	Calcium-dependent cell-cell adhesion via plasma membrane cell adhesion molecules	0.00	0.67
	GO:0005080	Protein kinase C binding	0.00	0.67
Control *vs.* OV-RACK1	GO:0051301	Cell division	6.63E-11	1.69E-07
	GO:0000082	G1/S transition of mitotic cell cycle	8.42E-05	0.01
	GO:0006281	DNA repair	3.29E-06	0.00

GSEA, gene set enrichment analysis; GO, gene ontology; MC, magnesium cantharidate; OV-RACK1, overexpression of receptor for activated C kinase 1.

Table 6. Enrichment analysis of GSEA/KEGG genes associated with cell proliferation, as well as apoptosis between different SK-Hep-1 cell treatment groups

Group	ID	Description	Pval	Padj
Control *vs.* MC	map03050	Proteasome	0.00	0.72
	map03420	Nucleotide excision repair	0.03	1.00
	map04621	NOD-like receptor signaling pathway	0.01	0.72
OV-RACK1 *vs.* OV-RACK1+MC	map04216	Ferroptosis	0.00	0.76
	map03008	Ribosome	1.00	1.00
	map04620	Toll-like receptor signaling pathway	0.03	0.85
Control *vs.* OV-RACK1	map04110	Cell cycle	0.01	0.01
	map03030	DNA replication	0.00	0.12
	map03420	Nucleotide excision repair	0.01	0.22

GSEA, gene set enrichment analysis; KEGG, Kyoto Encyclopedia of Genes and Genomes; MC, magnesium cantharidate; OV-RACK1, overexpression of receptor for activated C kinase 1; Pval, *P* value; Padj, adjusted *P* value; NOD, nucleotide-binding oligomerization domain; DNA, deoxynucleic acid.

sponse [31, 32]. The results of molecular docking indicated that the minimum binding energy between RACK1 and MC was -5.8 kcal/mol, which is lower than -5.0 kcal/mol, which suggested a strong interaction between MC and RACK1. Our results showed that MC significantly inhibited the expression of RACK1 in Huh-7 and SK-Hep-1 cells. Additionally, MC significantly inhibited cell viability and proliferation, and promoted apoptosis in RACK1-overexpressing or normal Huh-7 and SK-Hep-1 cells. Furthermore, MC treatment significantly inhibited the growth of liver cancer subcutaneous graft tumors in nude mice. Our findings revealed the potential of MC as an anti-HCC traditional Chinese medicine. Moreover, our results suggested that MC exerts anticancer effects by inhibiting RACK1 expression. However, further studies are needed to investigate the mechanisms underlying the anti-HCC effects of MC.

RNA-seq analysis revealed that CTBP1-AS2, CFAP298-TCP10L, and HSPE1-MOB4 may have significant roles in the RACK1- and MC-mediated regulation of liver cancer progression. In the context of HCC, TCGA data analysis has confirmed upregulated CTBP1-AS2 expression and its involvement in promoting HCC cell prolifera-

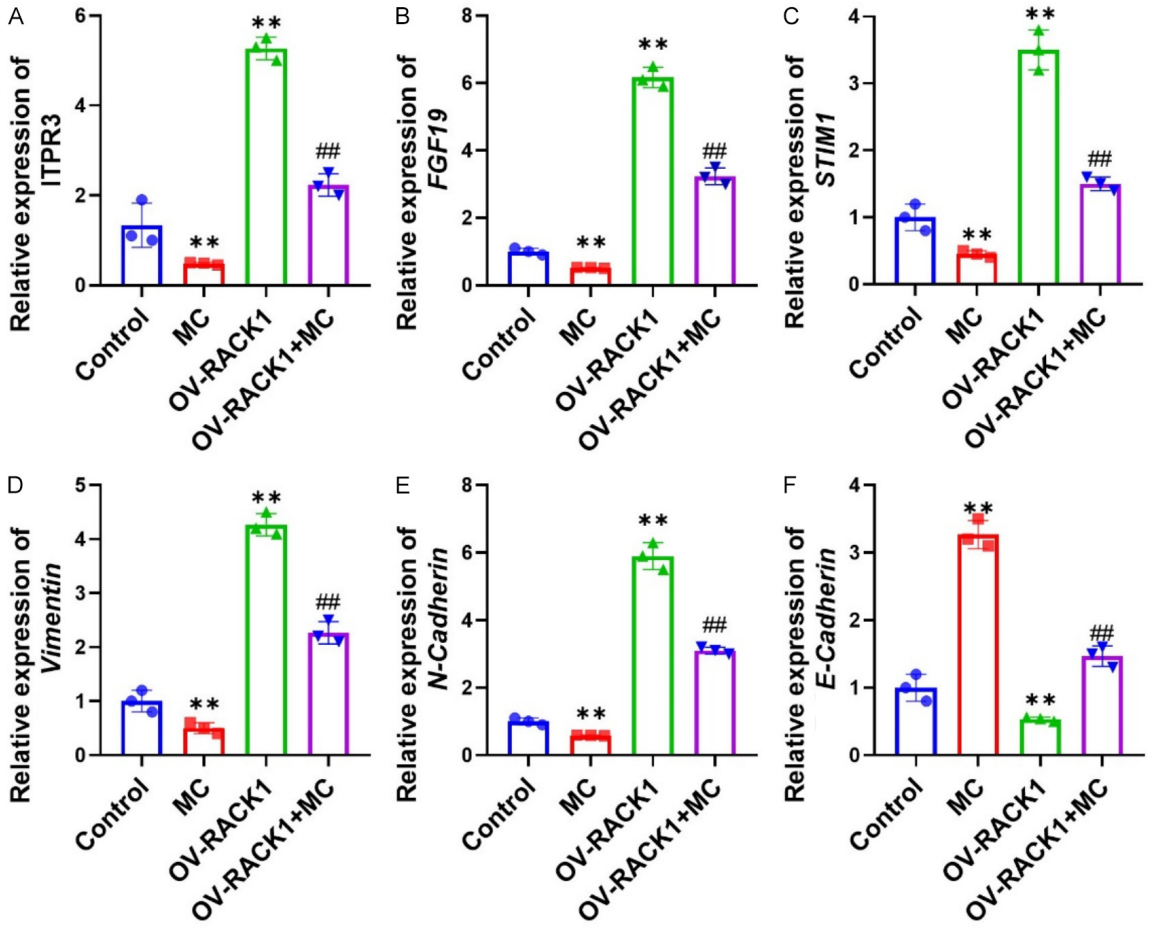

Figure 10. Expression analysis of calcium ion transport, ion channels, and cell adhesion pathway. (A-F) qRT-PCR was used to detect the expression of ITPR3 (A), FGF19 (B), STIM1 (C), vimentin (D), N-cadherin (E), and E-cadherin (F) mRNA expression in SK-Hep-1 cell (n=3). **compared to the control group (P<0.01). ##compared to the OV-RACK1 group (P<0.01).

tion by regulation of the miR-623/Cyclin D1 axis [33]. Moreover, Liu et al. [34] reported that CTBP1-AS2 expression is markedly elevated in HCC tissues and cell lines. They demonstrated that CTBP1-AS2 functions as a molecular sponge for miR-195-5p, thereby increasing CEP55 levels and promoting the oncogenic progression of HCC. In the current study, MC significantly downregulated the expression of CTBP1-AS2 in OV-RACK1 and normal SK-Hep-1 cells. Moreover, our results also demonstrated that MC significantly upregulated the expression of CFAP298-TCP10L and downregulated the expression of HSPE1-MOB4 in OV-RACK1 SK-Hep-1 cells. However, few studies have investigated the roles of CFAP298-TCP10L and HSPE1-MOB4 in liver cancer, which may be a future research direction. Based on previous studies, we speculated that MC exerted anticancer effects by targeting RACK1, thereby modulating the expression of CTBP1-AS2, CFAP298-TCP10L, and HSPE1-MOB4. However, further studies are required to investigate the relationship between MC and CTBP1-AS2, CFAP298-TCP10L, and HSPE1-MOB4 expression.

GO/KEGG results showed that RACK1 overexpression increased the expression of genes related to cell differentiation, DNA replication, DNA damage repair, and the cell cycle, thereby promoting cell proliferation. MC treatment increases the expression of genes related to calcium ion channels, cell adhesion, and protein binding to promote cell metabolism. The results of GSEA similarly showed that the functions of genes expressed after RACK1 overexpression were primarily related to the DNA double helix, DNA replication, DNA repair, and cell cycle, whereas the functions of genes expressed

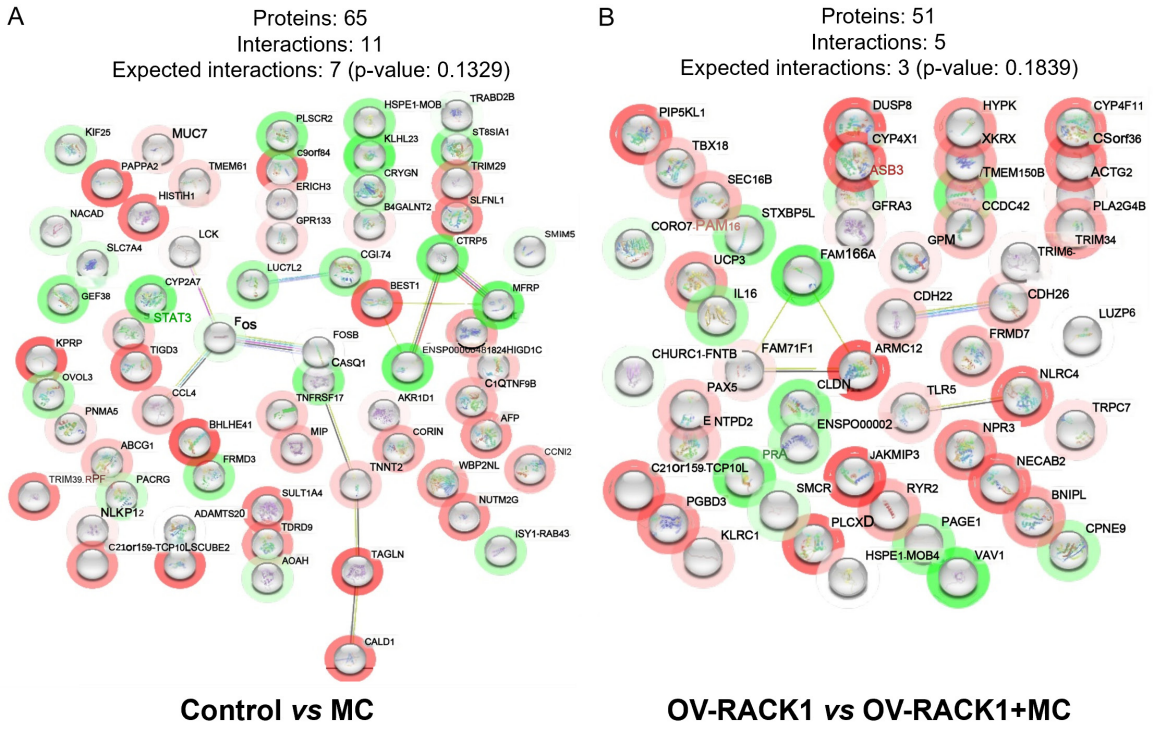
A
Proteins: 65
Interactions: 11
Expected interactions: 7 (p-value: 0.1329)
B
Proteins: 51
Interactions: 5
Expected interactions: 3 (p-value: 0.1839)
Control vs MC
OV-RACK1 vs OV-RACK1+MC

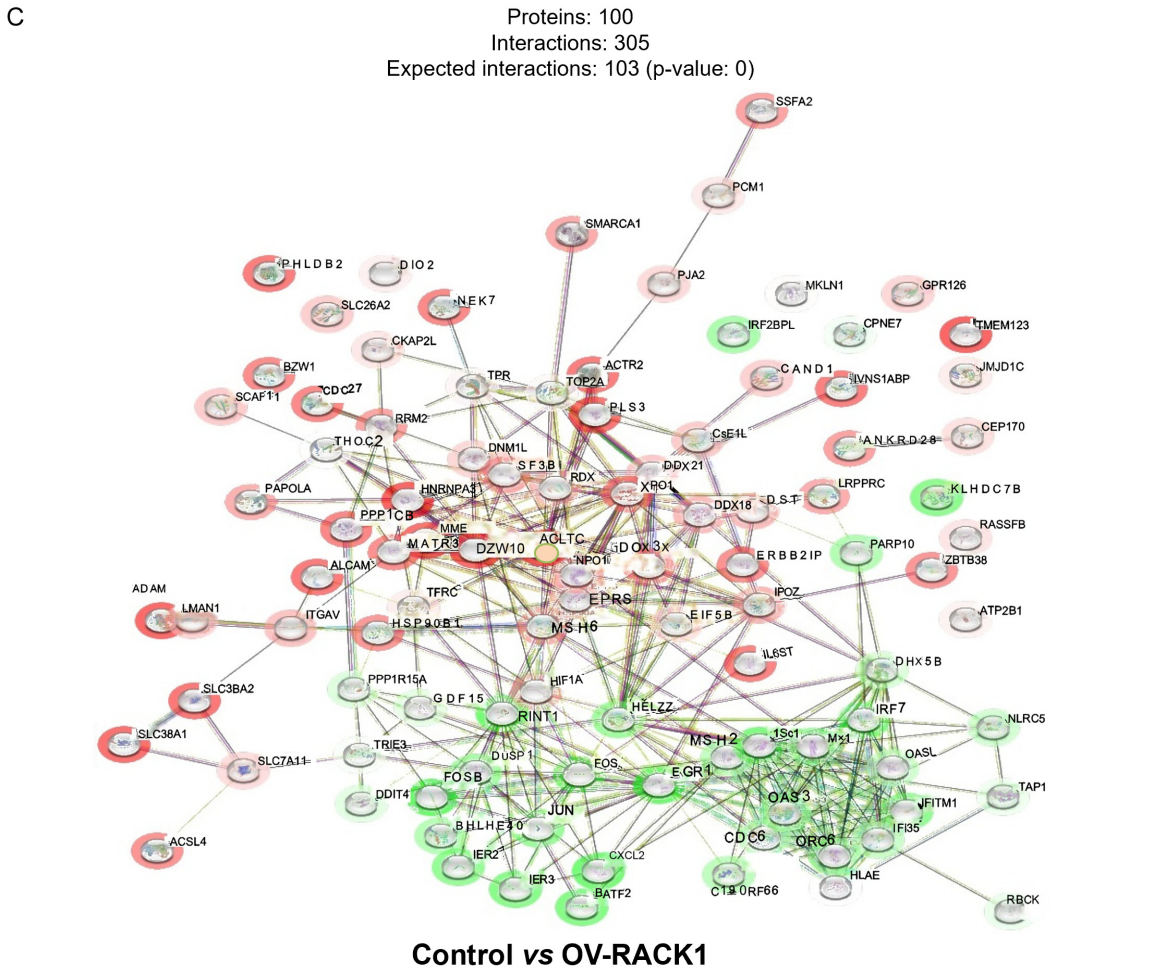
C
Proteins: 100
Interactions: 305
Expected interactions: 103 (p-value: 0)
Control vs OV-RACK1

Figure 11. Analysis of PPI protein interaction network between different SK-Hep-1 cell treatment groups. A. SK-Hep-1 control group *vs.* MC-treated group. B. RACK1 overexpression group *vs.* RACK1 overexpression +MC group. C. SK-Hep-1 control group *vs.* RACK1 overexpression group. *vs.*: versus.

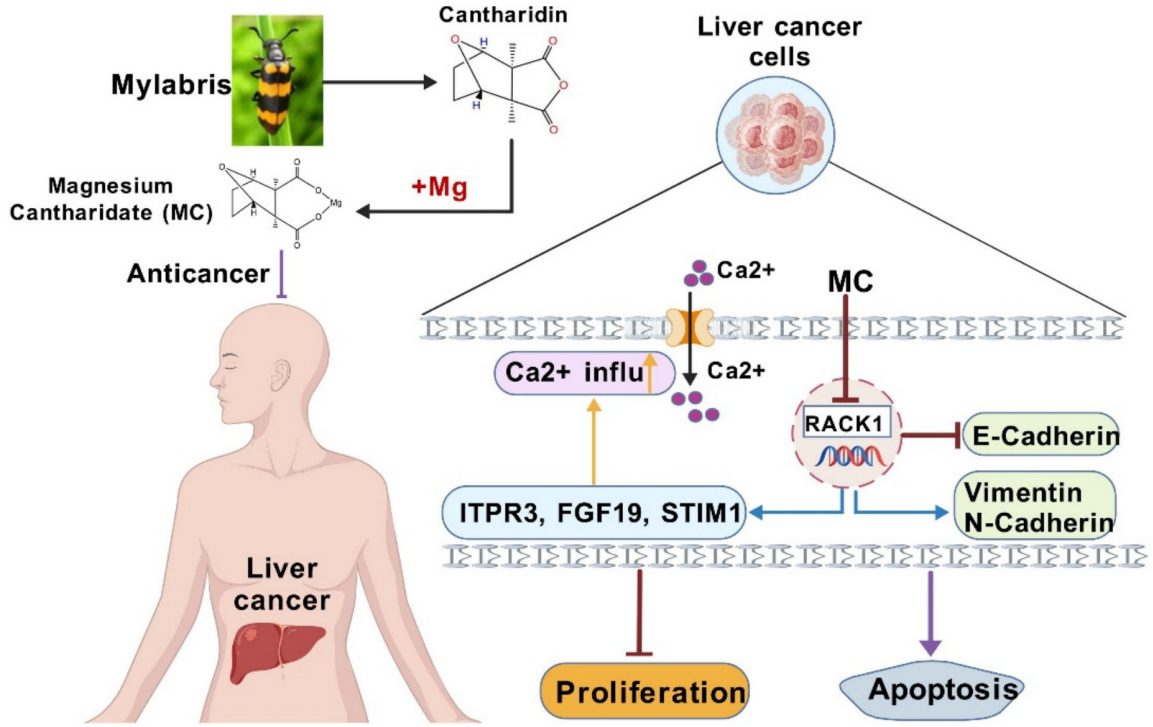

Figure 12. Magnesium cantharidate (MC) inhibits liver cancer cell proliferation and promotes apoptosis by targeting receptor for activated C kinase (RACK1).

after MC treatment were primarily related to iron ion and chloride transport, cell adhesion, nucleotide excision repair, and inflammation. In addition, PPI analysis revealed that protein expression during cell proliferation and DNA amplification were more active after RACK1 overexpression and that protein activity during cell metabolism increased after MC treatment.

Inositol 1,4,5-trisphosphate receptors (ITPRs) serve as intracellular Ca^{2+} channels in hepatocytes in hepatocytes. In particular, ITPR3 is undetectable or exists at low levels in normal hepatocytes, but it is highly expressed in HCC tissues [35]. Wang et al. [36] demonstrated that FGF19/FGFR4 signaling could activate store-operated Ca^{2+} entry (SOCE) through the PLCγ and extracellular signal-regulated kinase 1 and 2 pathways. STIM1-triggered SOCE is the major route for Ca^{2+} influx into nonexcitable cells, including HCC cells [37]. A recent study demonstrated that using a pharmacological inhibitor of SOCE in combination with STIM1 small interfering RNA treatment could reduce tumor metastasis in breast cancer animal models [38]. Vimentin, N-cadherin and E-cadherin are significantly associated with cell invasion and migration in liver cancer [39]. Experimental evidence demonstrated that restoring E-cadherin expression in cancer cells lacking E-cadherin can inhibit tumor progression and prevent invasion [40]. In this study, qRT-PCR results demonstrated that RACK1 overexpression significantly facilitated ITPR3, FGF19, STIM1, vimentin, and N-cadherin expression and inhibited E-cadherin expression, whereas MC treatment reversed the effects of RACK1 overexpression in SK-Hep-1 cells. Based on these results and biosignature analysis, we speculate that MC may affect the survival of liver cancer cells by regulating DNA damage repair, cell cycle, and ion channels. These results further confirm that MC exerts its anticancer effects through multiple pathways.

In conclusion, our study established a significant association between RACK1 expression and key clinicopathologic features of liver can-

cer, including tissue type, survival, stage, and TP53 mutations. RACK1 enhances the viability and proliferation of liver cancer cells while inhibiting apoptosis. These results suggest that RACK1 is a marker for liver cancer development and a promising therapeutic target. Moreover, our findings indicated that MC exhibits anti-liver cancer properties by promoting apoptosis and suppressing the viability and proliferation of liver cancer cells (**Figure 12**). MC had a pronounced counteractive effect on the procarcinogenic impact of RACK1, suggesting that RACK1 is a target for the anti-liver cancer action of MC. Nonetheless, these promising results are limited by the lack of clinical trial data, emphasizing the need for further studies in liver cancer.

Acknowledgements

This research was supported by the National Natural Science Foundation of China (Beijing, China; grant no. 82260812) and the Guizhou Provincial Science and Technology Program (Guiyang, China; grant no. ZK[2022]615).

Disclosure of conflict of interest

None.

Address correspondence to: Rong Yan and Lingjun Wang, College of Basic Medicine, Zunyi Medical University, 1 Campus Road, Xinpu New District, Zunyi 563000, Guizhou, China. E-mail: yanrong@zmu.edu.cn (RY); wanglingjun@zmu.edu.cn (LJW)

References

[1] Siegel RL, Miller KD, Wagle NS and Jemal A. Cancer statistics, 2023. CA Cancer J Clin 2023; 73: 17-48.

[2] Liu D and Song T. Changes in and challenges regarding the surgical treatment of hepatocellular carcinoma in China. Biosci Trends 2021; 15: 142-147.

[3] Brown ZJ, Tsilimigras DI, Ruff SM, Mohseni A, Kamel IR, Cloyd JM and Pawlik TM. Management of hepatocellular carcinoma: a review. JAMA Surg 2023; 158: 410-420.

[4] Dan H, Liu S, Liu J, Liu D, Yin F, Wei Z, Wang J, Zhou Y, Jiang L, Ji N, Zeng X, Li J and Chen Q. RACK1 promotes cancer progression by increasing the M2/M1 macrophage ratio via the NF-kappaB pathway in oral squamous cell carcinoma. Mol Oncol 2020; 14: 795-807.

[5] Yoshino Y and Chiba N. Roles of RACK1 in centrosome regulation and carcinogenesis. Cell Signal 2022; 90: 110207.

[6] Ou H, Wang L, Xi Z, Shen H, Jiang Y, Zhou F, Liu Y and Zhou Y. MYO10 contributes to the malignant phenotypes of colorectal cancer via RACK1 by activating integrin/Src/FAK signaling. Cancer Sci 2022; 113: 3838-3851.

[7] Yao F, Long LY, Deng YZ, Feng YY, Ying GY, Bao WD, Li G, Guan DX, Zhu YQ, Li JJ and Xie D. RACK1 modulates NF-kappaB activation by interfering with the interaction between TRAF2 and the IKK complex. Cell Res 2014; 24: 359-371.

[8] Yu Z, Jiang X, Qin L, Deng H, Wang J, Ren W, Li H, Zhao L, Liu H, Yan H, Shi W, Wang Q, Luo C, Long B, Zhou H, Sun H and Jiao Z. Correction: a novel UBE2T inhibitor suppresses Wnt/beta-catenin signaling hyperactivation and gastric cancer progression by blocking RACK1 ubiquitination. Oncogene 2021; 40: 2622-2623.

[9] Cao XX, Xu JD, Liu XL, Xu JW, Wang WJ, Li QQ, Chen Q, Xu ZD and Liu XP. RACK1: a superior independent predictor for poor clinical outcome in breast cancer. Int J Cancer 2010; 127: 1172-1179.

[10] Li X, Xiao Y, Fan S, Xiao M, Wang X, Chen X, Li C, Zong G, Zhou G and Wan C. RACK1 overexpression associates with pancreatic ductal adenocarcinoma growth and poor prognosis. Exp Mol Pathol 2016; 101: 176-186.

[11] Chen L, Min L, Wang X, Zhao J, Chen H, Qin J, Chen W, Shen Z, Tang Z, Gan Q, Ruan Y, Sun Y, Qin X and Gu J. Loss of RACK1 promotes metastasis of gastric cancer by inducing a miR-302c/IL8 signaling loop. Cancer Res 2015; 75: 3832-3841.

[12] Guo Y, Wang W, Wang J, Feng J, Wang Q, Jin J, Lv M, Li X, Li Y, Ma Y, Shen B and Zhang J. Receptor for activated C kinase 1 promotes hepatocellular carcinoma growth by enhancing mitogen-activated protein kinase kinase 7 activity. Hepatology 2013; 57: 140-151.

[13] Cao J, Zhao M, Liu J, Zhang X, Pei Y, Wang J, Yang X, Shen B and Zhang J. RACK1 promotes self-renewal and chemoresistance of cancer stem cells in human hepatocellular carcinoma through stabilizing nanog. Theranostics 2019; 9: 811-828.

[14] Wu J, Meng J, Du Y, Huang Y, Jin Y, Zhang J, Wang B, Zhang Y, Sun M and Tang J. RACK1 promotes the proliferation, migration and invasion capacity of mouse hepatocellular carcinoma cell line in vitro probably by PI3K/Rac1 signaling pathway. Biomed Pharmacother 2013; 67: 313-319.

[15] Zou YH, Li XD, Zhang QH and Liu DZ. RACK1 silencing induces cell apoptosis and inhibits cell proliferation in hepatocellular carcinoma MHCC97-H cells. Pathol Oncol Res 2018; 24: 101-107.

[16] Zhu M, Shi X, Gong Z, Su Q, Yu R, Wang B, Yang T, Dai B, Zhan Y, Zhang D and Zhang Y. Can-

tharidin treatment inhibits hepatocellular carcinoma development by regulating the JAK2/STAT3 and PI3K/Akt pathways in an EphB4-dependent manner. Pharmacol Res 2020; 158: 104868.
[17] Yan J, Deng XL, Ma SQ, Hui Li Y, Gao YM, Shi GT and Wang HS. Cantharidin suppresses hepatocellular carcinoma development by regulating EZH2/H3K27me3-dependent cell cycle progression and antitumour immune response. BMC Complement Med Ther 2023; 23: 160.
[18] Lan HY, An P, Liu QP, Chen YY, Yu YY, Luan X, Tang JY and Zhang H. Aidi injection induces apoptosis of hepatocellular carcinoma cells through the mitochondrial pathway. J Ethnopharmacol 2021; 274: 114073.
[19] An P, Lu D, Zhang L, Lan H, Yang H, Ge G, Liu W, Shen W, Ding X, Tang D, Zhang W, Luan X, Cheng H and Zhang H. Synergistic antitumor effects of compound-composed optimal formula from Aidi injection on hepatocellular carcinoma and colorectal cancer. Phytomedicine 2022; 103: 154231.
[20] Liu Y, Li X, Zou Q, Liu L, Zhu X, Jia Q, Wang L and Yan R. Inhibitory effect of magnesium cantharidate on human hepatoma SMMC-7721 cell proliferation by blocking MAPK signaling pathway. Xi Bao Yu Fen Zi Mian Yi Xue Za Zhi 2017; 33: 347-351.
[21] Tan XY, Yan R, Liu Y, Liu L, Wang LJ and Li XF. Effect of magnesium cantharidinate on the transcriptome of human hepatoma cell line SMMC-7721. Chinese Traditional Patent Medicine 2018; 40: 691-695.
[22] Yan R, Liu Y, Zhu XT, Yi XF, Liu L and Li XF. Effect of magnesium cantharidate on hepatocellular carcinoma SMMC-7721 cells and subcutaneous hepatocellular SMMC-7721 carcinoma transplantation tumors in nude mice. Chinese Journal of Applied Entomology 2015; 52: 477-485.
[23] Yan R, Liu Y, Zhu XT, Yi XF, Liu L and Li XF. Effect of different cantharidin materials on proliferation of human hepatocellular carcinoma cells HepG2. Journal of Modern Medicine & Health 2015; 31: 3209-3211.
[24] Wang Z, Huang YX, He TM, Tan XY, Li XF, Liu Y and Yan R. Magnesium cantharidate suppresses PP2A and ERK1/2 pathway to inhibit hepatocellular carcinoma cells. Toxicology Advances 2024; 6: 4.
[25] Buoso E, Masi M, Long A, Chiappini C, Travelli C, Govoni S and Racchi M. Ribosomes as a nexus between translation and cancer progression: focus on ribosomal receptor for activated c kinase 1 (RACK1) in breast cancer. Br J Pharmacol 2022; 179: 2813-2828.
[26] Xu C, Li YM, Sun B, Zhong FJ and Yang LY. GNA14's interaction with RACK1 inhibits hepatocellular carcinoma progression through reducing MAPK/JNK and PI3K/AKT signaling pathway. Carcinogenesis 2021; 42: 1357-1369.
[27] Wu H, Song S, Yan A, Guo X, Chang L, Xu L, Hu L, Kuang M, Liu B, He D, Zhao R, Wang L, Wu X, Gu J and Ruan Y. RACK1 promotes the invasive activities and lymph node metastasis of cervical cancer via galectin-1. Cancer Lett 2020; 469: 287-300.
[28] Tian R, Tian J, Zuo X, Ren S, Zhang H, Liu H, Wang Z, Cui Y, Niu R and Zhang F. RACK1 facilitates breast cancer progression by competitively inhibiting the binding of beta-catenin to PSMD2 and enhancing the stability of beta-catenin. Cell Death Dis 2023; 14: 685.
[29] Chen J, Tang J, Wang H, Mei J, Wei X, Qin X, Lin Q, Huang Z, Tang W and Luo T. Isobutyric acid promotes colorectal cancer metastasis through activating RACK1. Cancer Sci 2023; 114: 3900-3913.
[30] Huang M, Xiao J, Yan C, Wang T and Ling R. USP41 promotes breast cancer via regulating RACK1. Ann Transl Med 2021; 9: 1566.
[31] Liu Y and Feng N. Nanocarriers for the delivery of active ingredients and fractions extracted from natural products used in traditional Chinese medicine (TCM). Adv Colloid Interface Sci 2015; 221: 60-76.
[32] Zhang J, Zou L, Li Q, Wu H, Sun Z, Xu X, Shi L, Sun Z and Ma G. Carbon dots derived from traditional chinese medicines with bioactivities: a rising star in clinical treatment. ACS Appl Bio Mater 2023; 6: 3984-4001.
[33] Wang M and Zhao H. LncRNA CTBP1-AS2 promotes cell proliferation in hepatocellular carcinoma by regulating the miR-623/cyclin D1 axis. Cancer Biother Radiopharm 2020; 35: 765-770.
[34] Liu LX, Liu B, Yu J, Zhang DY, Shi JH and Liang P. SP1-induced upregulation of lncRNA CTBP1-AS2 accelerates the hepatocellular carcinoma tumorigenesis through targeting CEP55 via sponging miR-195-5p. Biochem Biophys Res Commun 2020; 533: 779-785.
[35] Guerra MT, Florentino RM, Franca A, Lima Filho AC, Dos Santos ML, Fonseca RC, Lemos FO, Fonseca MC, Kruglov E, Mennone A, Njei B, Gibson J, Guan F, Cheng YC, Ananthanarayanan M, Gu J, Jiang J, Zhao H, Lima CX, Vidigal PT, Oliveira AG, Nathanson MH and Leite MF. Expression of the type 3 InsP(3) receptor is a final common event in the development of hepatocellular carcinoma. Gut 2019; 68: 1676-1687.
[36] Wang J, Zhao H, Zheng L, Zhou Y, Wu L, Xu Y, Zhang X, Yan G, Sheng H, Xin R, Jiang L, Lei J, Zhang J, Chen Y, Peng J, Chen Q, Yang S, Yu K, Li D, Xie Q and Li Y. FGF19/SOCE/NFATc2 sig-

naling circuit facilitates the self-renewal of liver cancer stem cells. Theranostics 2021; 11: 5045-5060.
[37] Zhao H, Yan G, Zheng L, Zhou Y, Sheng H, Wu L, Zhang Q, Lei J, Zhang J, Xin R, Jiang L, Zhang X, Chen Y, Wang J, Xu Y, Li D and Li Y. STIM1 is a metabolic checkpoint regulating the invasion and metastasis of hepatocellular carcinoma. Theranostics 2020; 10: 6483-6499.
[38] Chen JP, Luan Y, You CX, Chen XH, Luo RC and Li R. TRPM7 regulates the migration of human nasopharyngeal carcinoma cell by mediating Ca(2+) influx. Cell Calcium 2010; 47: 425-432.
[39] Zheng Y, Huang C, Lu L, Yu K, Zhao J, Chen M, Liu L, Sun Q, Lin Z, Zheng J, Chen J and Zhang J. STOML2 potentiates metastasis of hepatocellular carcinoma by promoting PINK1-mediated mitophagy and regulates sensitivity to lenvatinib. J Hematol Oncol 2021; 14: 16.
[40] Navarro P, Gomez M, Pizarro A, Gamallo C, Quintanilla M and Cano A. A role for the E-cadherin cell-cell adhesion molecule during tumor progression of mouse epidermal carcinogenesis. J Cell Biol 1991; 115: 517-533.